

Augmenting transcriptome assembly combinatorially

Prachi Jain¹⁺, Neeraja M Krishnan¹⁺ and Binay Panda^{1,2*}

¹Ganit Labs, Bio-IT Centre, Institute of Bioinformatics and Applied Biotechnology, Bangalore, India

²Strand Life Sciences, Hebbal, Bangalore, India

⁺equal contribution

*corresponding author (binay@ganitlabs.in)

Abstract

RNA-seq allows detection and precise quantification of transcripts, provides comprehensive understanding of exon/intron boundaries, aids discovery of alternatively spliced isoforms and fusion transcripts along with measurement of allele-specific expression. Researchers interested in studying and constructing transcriptomes, especially for non-model species, often face the conundrum of choosing from a number of available *de novo* and genome-guided assemblers. A comprehensive comparative study is required to assess and evaluate their efficiency and sensitivity for transcript assembly, reconstruction and recovery. None of the popular assembly tools in use today achieves requisite sensitivity, specificity or recovery of full-length transcripts on its own. Hence, it is imperative that methods be developed in order to augment assemblies generated from multiple tools, with minimal compounding of error. Here, we present an approach to combinatorially augment transcriptome assembly based on a rigorous comparative study of popular *de novo* and genome-guided transcriptome assembly tools.

Introduction

High-throughput technology has changed our understanding of many facets of biology, from diseases to plant genetics, and to synthetic biology. The advent of DNA microarrays in the 90's ushered an era of high-throughput genome-wide gene expression profiling studies. DNA microarray, although a powerful technique, is dependent on gene annotation, and hence genome sequence information. This is circumvented by RNA sequencing (RNA-seq), which uses next-generation sequencing instruments. This shift from the semi-quantitative, hybridization-based approaches, as in DNA microarrays, to the quantitative, sequencing-based approaches has tremendously facilitated gene expression analysis. RNA-seq experiments yield additional information on transcriptome characterization and quantification, including strand-specificity, mapping of fusion transcripts, small RNA identification and alternate splicing information.

A number of tools have been developed for transcriptome assembly in the past. They are classified under *de novo* and genome-guided assembly categories. Trinity, SOAPdenovo-Trans, Oases and Trans-ABYSS are *de novo* tools, while TopHat-Cufflinks, and Genome guided Trinity fall under the second category. *De novo* assembly tools create short contigs from overlapping reads, which are extended based on insert size estimates. They could be based on either construction of *de Bruijn* graphs (using *k*-mers for short reads) or use overlap-layout-consensus (for longer reads) algorithms. In Genome guided Trinity, the reads are aligned to the genome and partitioned into read clusters, which are individually assembled using Trinity. TopHat-Cufflinks is an aligner cum assembly pipeline, involving spliced read alignment to the genome and subsequent assembly of these aligned reads into transcripts. The genome template and read pairing are utilized here to produce full-length or near full-length transcripts. Studies have identified *k-mer* size as an important parameter for short-read transcriptome assembly quality. The theoretical calculation on assembling transcriptomes based on *k-mer* size (a lower or higher *k-mer* length for low- or high-expressed genes respectively) has also been backed by experimental evidence. The *k-mer* length depends on the genome complexity, sequencing depth and sequencing error. One can take a decision on *k-mer* length depending on desired transcript diversity vs continuity of a given transcriptome.

Varying expression levels among genes, presence of homologues and spliced isoforms increase the complexity in transcriptome assembly. Availability of genome sequence can aid the performance of transcriptome assembly process. In its absence, genomes of closely related organisms can be used for transcriptome assemblies. Both *de novo* and genome-guided approaches have their own strengths and one can think of combining data from both to achieve higher sensitivity. However, the process of combining assemblies from multiple assemblers is not error free and may produce false assemblies. In the current paper, we first describe a detailed analysis of existing *de novo* and genome-guided tools and then determine the best combination of tools that can be used to augment the process of assembly while keeping the false assemblies to a minimum.

Materials and Methods

Simulating RNA-seq reads

The *Arabidopsis thaliana* (TAIR10) complete genome sequence, co-ordinates for genes and transposons were downloaded from ftp://ftp.arabidopsis.org/home/tair/Genes/TAIR10_genome_release and the GFF file was parsed to obtain exonic coordinates. These were used to simulate Illumina-like RNA-seq reads using Flux-simulator (FS-nightly-build_1.1.1-20121119021549) with the following options supplied within a parameter file (Supplementary Methods): NB_MOLECULES 5000000 , SIZE_DISTRIBUTION N(300,30) , READ_NUMBER 4000000 , READ_LENGTH 76 , PAIRED_END YES , ERR_FILE 76. The resultant Illumina-like reads were split into 2 fastq files corresponding to read1 and read2 using a Python script from the Galaxy tool suite (Supplementary Methods).

Zebrafish transcriptome data

RNA-seq reads for the zebrafish, *Danio rerio*, (2dpf) embryo were downloaded from SRA (ERR003998) . The zebrafish genome (Zv9) downloaded from Ensemble was used for genome-guided transcriptome assembly. The transcripts for hox gene cluster (listed in Table 2 in Corredor-Adamez et al. 2005) were downloaded from ENSEMBL, and used to identify hox-related genes from the assemblies through Megablast. We focused on read-covered shared and unique regions of the hox gene cluster.

Read assembly

The simulated and *Danio rerio* reads were assembled using four *de novo* (Trinity, version r2012-06-08; Trans-ABYSS, version 1.3.2; Oases, version 0.2.08; SOAPdenovo-Trans, version 1.0 for simulated data and version 1.02 for *Danio rerio*) and two genome-guided (Tophat1, version 2.0.4 that uses Bowtie1 , version 0.12.8 and Cufflinks, version 2.0.0; Genome guided Trinity, version r2012-10-05 that uses GSNAP , version 2012-07-20 [V3] for simulated data and version 2013-03-31 [V5]) for zebrafish data in the process of transcriptome assembly pipelines. We used Trinity and Genome guided Trinity with a fixed kmer size of 25bp, Trans-ABYSS on ABYSS (version 1.3.3) multi-kmer assemblies (ranging from 20-64bp), Oases on Velvet (version 1.2.07) multi-kmer assemblies (every alternate kmer ranging from 19-71bp) and SOAPdenovo-Trans with a fixed kmer size of 23bp. We tested the Tophat2 (version 2.0.7 that uses Bowtie version 2.0.5)-Cufflinks pipeline on the simulated data but did not observe any difference in the assembly statistics compared to the Tophat1-Cufflinks pipeline that uses Bowtie1. All assemblers were run using default parameters (details in Supplementary Methods). However, we fixed the parameter for minimum length of assembled fragment as 76bp (equal to the length of the read). In the case of SOAPdenovo-Trans, contigs were used instead of scaffolds for all downstream analyses, as the minimum length cutoff could not be set for scaffolds.

In order to test whether we could augment the assembly of Trinity-predicted transcript fragments with those from Tophat1-Cufflinks, we used Megablast to map the Trinity transcript fragments against the Tophat1-Cufflinks transcripts, and then augmented Trinity assembly with those transcript fragments unique to Tophat1-Cufflinks assembly (see Supplementary Methods for details).

Redundancy removal using CD-HIT-EST

We used CD-HIT-EST (version 4.5.4) to remove redundancy in each assembly. It retained the longest sequence out of a cluster of sequences that shared at least 95% sequence similarity based on a word size of 8. Further details on the options used to run CD-HIT-EST are provided in Supplementary Methods.

Model Assembly

We defined all read-covered transcript regions (TAIR10 for simulated data and hox gene cluster for *Danio rerio*) as Model Assembly or MA as previously described in the report by Mundry et al 2012 .

Calculation of N50 and $N_{(MA)50}$ statistics for an assembly

N50 is defined as the minimum contig length for 50% of the assembly, after sorting the contigs in the descending order of their lengths. We calculated N50 values for all assemblies, MA and the TAIR10 simulated transcripts, pre- and post-CD-HIT-EST. We also calculated the N50 values for each assembler, while taking the MA cumulative size (bp) as the denominator instead of the respective assembly sizes. We termed these N50 values as the $N_{(MA)50}$.

Mapping assemblies to MA using Megablast

The assembled fragments (query) were mapped against the MA fragments (subject) using Megablast (blast+ version 2.2.26) with default parameters (Supplementary Methods). The Megablast hits were parsed in order to either maximize query coverage (to compute mis-assembly statistics) or maximize subject coverage (to compute

MA recovery statistics). This was done to choose the best hits and discard the partially overlapping hits when the unique coverage was lower than or equal to 10bp. The scripts used to remove nested and partial overlaps from Megablast hits are provided in Supplementary Methods.

Expression level bin categories

We estimated the average “per nucleotide coverage” (pnc) for all MA fragments, based on their read support as Number of reads multiplied by Read Length divided by MA fragment length. The MA fragments were then categorized into 8 expression level bins, B1 to B8, the pnc for each being: 1 for B1, >1 & ≤ 2 for B2, >2 & ≤ 3 for B3, >3 & ≤ 4 for B4, >4 & ≤ 5 for B5, >5 & ≤ 10 for B6, >10 & ≤ 30 for B7, and >30 for B8. We chose denser sampling for the lower pnc values and sparser sampling for the higher pnc values since we observed the distribution of MA fragments to be denser in the lower pnc categories.

Recovery of isoforms

Using simulated data, we obtained the MA equivalent for the exonic regions of isoform-bearing genes, and performed a Megablast search of the assemblies against it (Supplementary Methods). The Megablast hits were parsed to maximize subject coverage, after removing nested and partial overlaps (same as described earlier). For all assemblers, we calculated the number of exons recovered per isoform and the length recovery of each exon.

Results

We compared the performance of assemblers using a variety of assembly-based parameters (numbers and lengths of assembled fragments, N50, $N_{(MA)}50$ and extent of redundancy) and mapping parameters (mapping based recovery of MA fragments (numbers and lengths), mis-assembly, reliance on pnc) for isoforms and non-isoforms, and shared and unique transcript regions.

Assembly statistics

We simulated reads for the exonic regions of the *Arabidopsis thaliana* TAIR10 genome (see Methods for details) and obtained Illumina-like paired-end 76bp reads covering 15,532 transcripts. The transcript regions contiguously covered by reads were termed as Model Assembly (MA) fragments and were used as a valid reference for mapping the assemblies. A given transcript, therefore, comprised of one or more MA fragments, the shortest being 76 bp in length. We obtained 70,382 MA fragments from the 15,532 TAIR10 transcripts. The reads were assembled using Trinity, Trans-ABBySS, Oases, SOAPdenovo-Trans, Tophat1-Cufflinks and Genome guided Trinity (see Methods for details) with default parameters and a minimum of 76bp assembled fragment length. We compared the numbers of assembled fragments, the minimum and maximum fragment lengths, their respective length frequency distributions, the N50 and $N_{(MA)}50$ statistics for the six assemblers, before and after eliminating redundancy in the assembly using CD-HIT-EST.

The total number of assembled fragments varied widely across the six assemblers (Table 1). We observed a 4- and ~1.5-fold reduction in assembly size post redundancy removal for Trans-ABBySS and Oases, respectively (Table 1). The shortest fragment reported by all assemblers was 76bp (as fixed by the minimum reporting length threshold). The range of fragments at the long end varied across assemblers with the longest for Tophat1-Cufflinks at 10,502 bp (same as the maximum MA fragment length, Table 1). This was expected since Tophat1-Cufflinks is a genome-guided assembler that allows recovery of full length or near full length transcripts. For Trinity, genome guided Trinity and SOAPdenovo-Trans, we observed no difference pre- and post-redundancy removal across the entire distribution of assembled fragment lengths (Figure 1). However, Trans-ABBySS resulted in a higher number of longer redundant assembled fragments (Figure 1) and interestingly a low number of shorter assembled fragments. Like the results from the frequency distribution statistics for long- and short-assembled fragments, Trinity, genome guided Trinity and SOAPdenovo-Trans yielded N50 values closer to that of MA. However, Trans-ABBySS, Oases and TopHat1-Cufflinks yielded N50 numbers that were much higher than that of MA. After eliminating redundancy, the N50 values were not affected for most assemblers except for Trans-ABBySS (Table 1). In contrast, the $N_{(MA)}50$ values, which are not dependent on the size of any assembly, were lower than that of the MA, for Trinity, Genome guided Trinity and SOAPdenovo-Trans, both before and after redundancy removal. For Trans-ABBySS and Oases, the $N_{(MA)}50$ values were relatively higher, and were reduced ~3 and ~1.5-fold respectively, after redundancy removal. The $N_{(MA)}50$ values were higher than that of the MA for Tophat1-Cufflinks, both before and after redundancy removal.

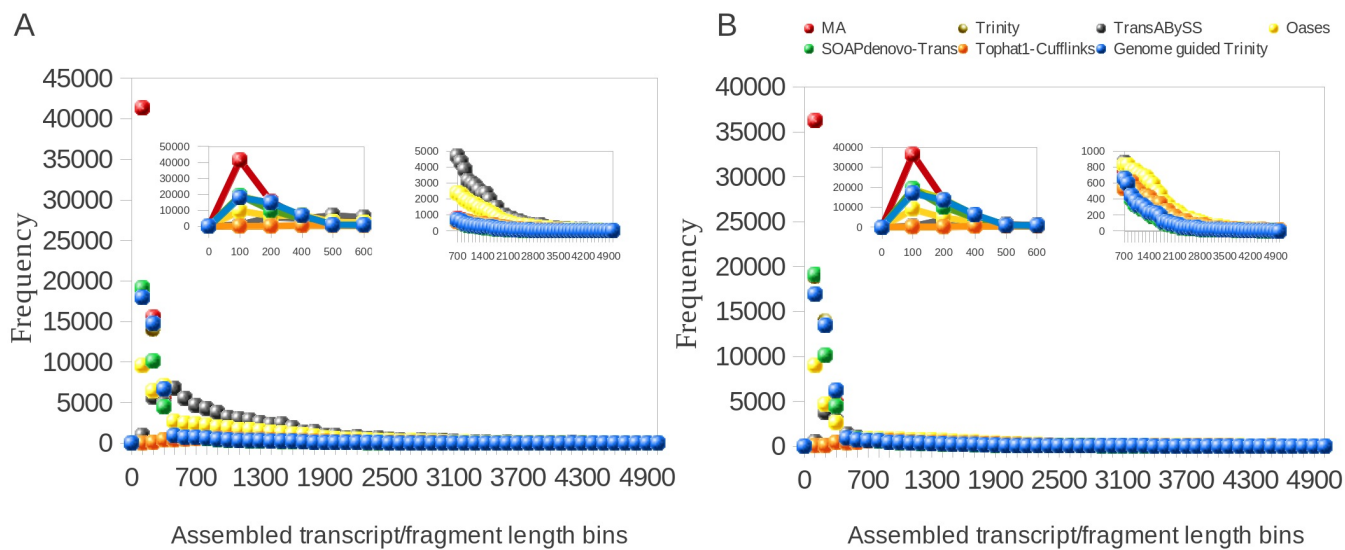


Figure 1: Frequency distribution of lengths (nt) of MA & assembled transcript fragments before (A) and after (B) CDHIT-EST.

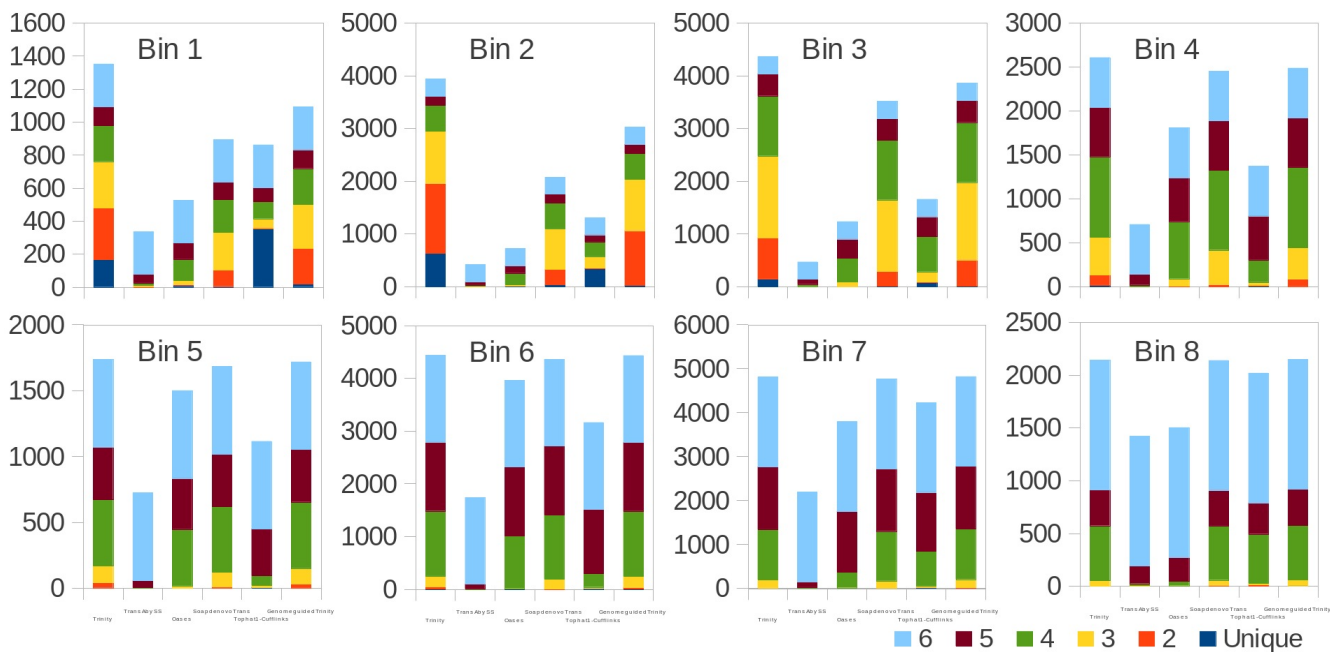


Figure 2: The number of recovered MA fragments in different expression bins.

Table 1: Assembly statistics pre- and post-CDHit-EST.

Pre CDHit-EST									
	TAIR10	Model	Trinity	Trans-	Oases	SOAP	Tophat1-	Genome	
	tran-	Assem-		ABySS		denovo-	Cufflinks	guided	
	scripts	bly (MA)				Trans		Trinity	
Total transcripts or fragments	15532	70382	45978	65594	52533	39533	8671	46064	
Transcriptome size (bp)	2.61E+07	1.67E+07	1.27E+07	6.62E+07	4.21E+07	1.02E+07	1.15E+07	1.27E+07	
N50 (bp)	1952	720	684	1390	1453	617	1624	646	
N(MA)50 (bp)	1952	720	264	2802	2519	114	1136	254	
Median transcript/fragment length (bp)	1456	85	115	804	523	103	1124	121	
Min. transcript/fragment length (bp)	201	76	76	76	76	76	76	76	
Max. transcript/fragment length (bp)	14623	10501	6888	7326	8128	6300	10502	7833	
Post-CDHit-EST									
	TAIR10	Model	Trinity	Trans-	Oases	SOAP	Tophat1-	Genome	
	tran-	Assem-		ABySS		denovo-	Cufflinks	guided	
	scripts	bly (MA)				Trans		Trinity	
Total transcripts or fragments	14615	62528	45281	16060	28051	39471	8395	42968	
Transcriptome size (bp)	2.45E+07	1.56E+07	1.21E+07	1.15E+07	1.85E+07	1.02E+07	1.11E+07	1.20E+07	
N50 (bp)	1951	788	627	1194	1485	617	1621	661	
N(MA)50 (bp)	1951	788	260	798	1680	155	1197	273	
Median transcript/fragment length (bp)	1451	87	113	477	216	103	1121	120	
Min. transcript/fragment length (bp)	201	76	76	76	76	76	76	76	
Max. transcript/fragment length (bp)	14623	10501	6888	7326	8128	6300	10502	7833	

Mapping-based statistics

MA fragments from TAIR10 transcripts corresponding to transposable elements and transcript isoforms, as per the GFF annotation, were not included in the expression level based binning. We excluded these elements since they have stretches of identical sequences, which posed a problem in assigning the pnc index and reliable mapping to the correct isoform and/or transposable element. Out of a total of 70,382 MA fragments, we were thus left with 46,805 fragments, which still had certain level of sub-sequence similarity, presumably arising from gene paralogs and SSRs. The numbers of MA fragments obtained in different expression bins were, 15,706 in B1 (the lowest expression bin), 9,722 in B2, 5,205 in B3, 2,797 in B4, 1,820 in B5, 4,522 in B6, 4,862 in B7 and 2,171 in B8 (the highest expression bin).

MA recovery statistics

The assembled transcript fragments from all assemblers were mapped to the MA using Megablast to assign common identifiers for comparisons. We compared the numbers and lengths of MA fragments recovered within expression bins, B1 to B8, using the best hits from Megablast. Trinity detected the highest number of MA fragments in B1 followed by Genome guided Trinity and SOAPdenovo-Trans (Figure 2). However, the number of unique transcripts detected was highest for Tophat1-Cufflinks, followed by Trinity for the lowest expression bin

B1 (Figure 2). The extent of overlapping between Trinity and either Genome guided Trinity or SOAPdenovo-Trans was 30% for the lowest expression bin B1. The numbers detected were highest for Trinity for all expression bins (B1-B8) with other assemblers showing recovery with increase in expression. In comparison to Trinity, for Oases and Trans-ABBySS the detection sensitivity increased with increased expression but the overall number of recovered MA fragments remained lower in all expression bins (Figure 2). Tophat1-Cufflinks showed a drop in its detection sensitivity from B1 to B2, and a steady rise thereafter. For all other assemblers, with the exception of Trans-ABBySS, we observed an increase in higher-order intersections proportional to the decrease in unique detections and lower order intersections across bins B2-B8 (Figure 2).

We observed that longer MA fragments tend to have higher read support, thus assigning them to the higher expression level bins (Supplementary Figure 1). The shorter MA fragments, however, got assigned to all expression level bins, as they had low-to-high read support (Supplementary Figure 1). Therefore, we decided to compare the length recovery across assemblers, for each expression level bin, in different MA fragment length categories (Figure 3). For the shortest length category, 76bp, the median length recovery was close to 100%, across all expression bins for all assemblers, with the exception of Trans-ABBySS (Figure 3). The outlier trend was highly variable across assemblers, and clustered closer to the median for SOAPdenovo-Trans, followed by Trinity and Genome guided Trinity. For Trinity, Trans-ABBySS, Oases and Genome guided Trinity, we observed the outliers clustering around ~40% length recovery (~30bp) for the MA fragments in the lowest expression bin that matched the word size for Megablast (28bp). The outliers in the lowest expression bin for Tophat1-Cufflinks and those in the highest expression bins for Oases spanned all the way from ~40% to the median. For the subsequent length categories, we observed a gradual increase in the median length recovery from as low as 20% to all the way upto 100%, with an increase in the expression levels. This gradual increase was also seen, to a minor extent, for the same bin across MA length categories, for most assemblers. Tophat1-Cufflinks showed a median recovery of 100% across all expression bins and all MA fragment length categories. The pattern of length recovery was similar for Trinity, SOAPdenovo-Trans and Genome guided Trinity across all the expression bins and MA fragment length categories. Overall, these three assemblers outperformed Trans-ABBySS and Oases in terms of higher median MA fragment length recovery and tighter distribution around the median (Figure 3).

Mis-assembly statistics

We used Megablast-based mapping to evaluate the accuracy of assembled fragments, and determine whether each assembled fragment belonged to a single MA source or was a chimera across multiple sources (mis-assembled). We classified the assembled fragments into three categories, $\geq 90\%$, between 60-90%, and $< 60\%$ based on the extent of their lengths mapped to any single MA fragment. They were further classified into various assembled length categories to check their relationship with assembly quality, before and after removing redundancy. Trans-ABBySS and Oases showed relatively higher number of mis-assembled fragments (between 60-90%, and $< 60\%$ mapping) in the 200-400bp and 500-600bp ranges respectively (Figure 4). In the case of Trans-ABBySS, the extent of mis-assembly decreased after removing redundancy, whereas in the case of Oases, it went up. We did not observe any difference in the extent of mis-assembly, pre- and post-redundancy removal, for any other assembler (Figure 4). The extent of mis-assembly was over-estimated with Tophat1-Cufflinks as it surpassed the length of the MA fragment (Table 1). For Trinity, SOAPdenovo-Trans and Genome guided Trinity, there was a clear trend of decreasing mis-assembly with increasing assembled fragment length (Figure 4). The degree of mis-assembly was lesser for SOAPdenovo-Trans than for Trinity or Genome guided Trinity for the shorter fragments.

Recovery of isoforms

Next, we compared the extent of recovery of known isoforms from the transcripts assembled with various assemblers. We had a total of 24,846 exons in the MA fragments corresponding to 2,970 isoforms. We mapped assembled fragments from all assemblers to these exons, using Megablast, and maximized exon coverage. Trinity, followed by Genome guided Trinity and SOAPdenovo-Trans had the highest numbers of isoforms in the 80-100% length recovery category (Figure 5). We observed a correlation between the median pnc for each recovery category and the numbers of exons recovered per isoform. The median pnc was in the range of 2-3 for unrecovered isoforms and 17-23 for those which were fully recovered or close to fully recovered by all assemblers. Trans-ABBySS and Oases, which showed a relatively lower recovery, correlated with a higher median pnc, suggesting a higher threshold of pnc needed for good recovery by those assemblers (Figure 5).

In order to test whether our understanding of isoform recovery from simulated reads holds true for a real dataset, we measured the recovery of shared and unique assembled transcripts for the shared and unique regions of the hox gene cluster in zebrafish (see Methods for details). We observed that across assemblers, Trinity, followed by Genome guided Trinity and SOAPdenovo-Trans recovered most and closer to full length

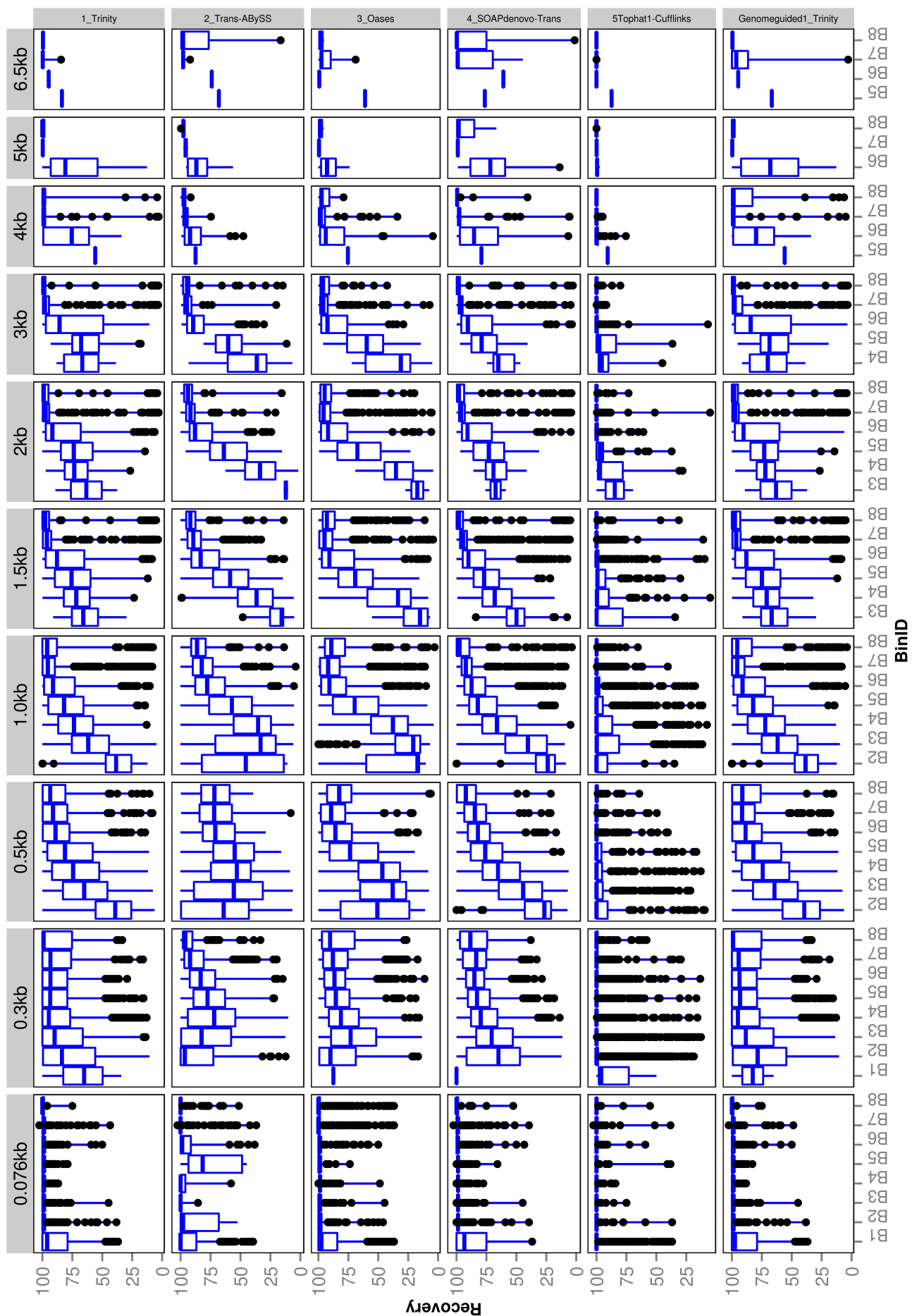


Figure 3: Recovered length (%) of MA fragments.

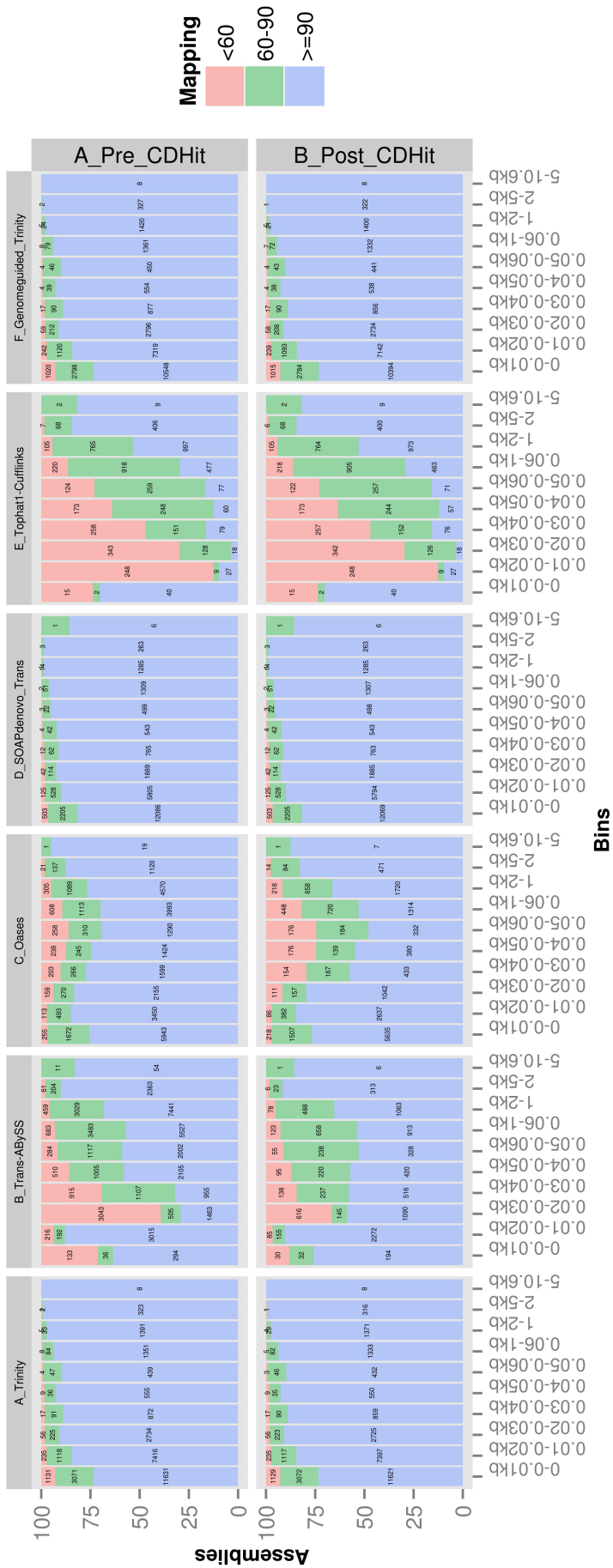


Figure 4: Assembly mapping statistics.

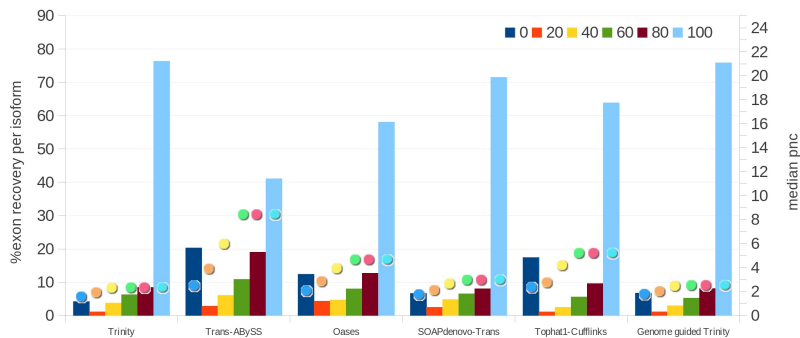


Figure 5: Isoform recovery statistics.

transcripts (Figures 6-8). Tophat1-Cufflinks recovered mostly full-length transcripts, but fewer in numbers. Trans-ABYSS and Oases recovered fewer and truncated transcripts. The length recovery (%) by all assemblers except Tophat1-Cufflinks displayed a dependency on pnc which was more obvious in the recovery of shared regions of transcripts, as expected due to a wider range of read depth (Figures 6-7).

Augmenting transcriptome assembly

Since each assembler produced a set of unique transcripts or fragments, we proceeded towards augmenting the assemblies, one with another. We ruled out most combinations of assemblers, and chose Trinity and Tophat1-Cufflinks, as Trinity produced most number of transcript fragments and TopHat-Cufflinks the most number of full-length transcripts. After aligning the Trinity transcript fragments to the Tophat1-Cufflinks transcripts, we obtained a cumulative size increase of 1.37 Mbp (~20% of original Trinity assembly size), unique to Tophat1-Cufflinks. We observed an increase of 1,377 in number of MA fragments and 5,23,127nt in total cumulative length recovered after augmenting Trinity transcript fragments with Tophat1-Cufflinks-specific transcript regions. Relaxing the stringency of Megablast word size, from 28 to lower, would have increased our MA length recovery further, at the expense of losing isoform reconstruction capability and sensitivity to variation in read-depth, maintained by the fragmented structure of Trinity transcriptome assembly. We further observed that the median length recovery for the augmented Trinity was overall better than Trinity by itself (Figure 9). For transcripts longer than 1500nt, this augmentation yielded full-length transcripts across all expression levels (Figure 9). Even for transcripts that are of sizes around 500nt, we saw the advantage of augmentation, at least for recovering more transcripts that are towards full length. The outliers were fewer in augmented Trinity than Tophat1-Cufflinks in all length categories. The improved recovery with augmented Trinity proved that an integrative approach was useful, particularly when one has access to genome in addition to the RNA-seq reads.

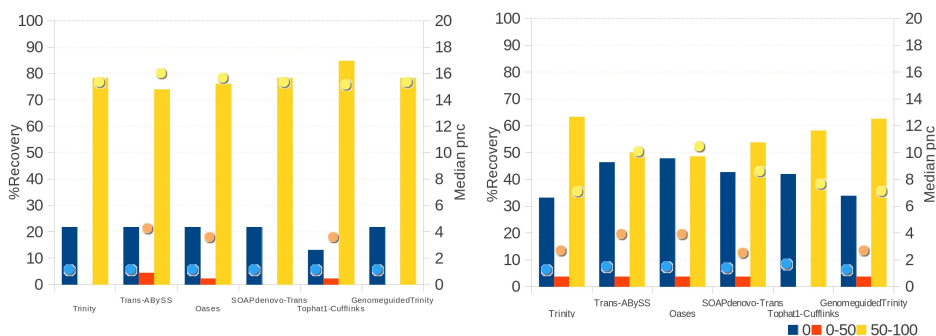


Figure 6: Recovery of transcripts in the zebrafish hox gene cluster.

Discussion

RNA-seq using next-generation sequencing is a powerful technology to understand the transcriptome of an organism. Although, genome guided assemblers like Tophat-Cufflinks can assemble full length transcripts, most *de novo* approaches and even Genome guided Trinity, where the genome is used only to partition the RNA-seq reads, are useful in detecting novel transcripts. In our comparative study, we found that each assembler

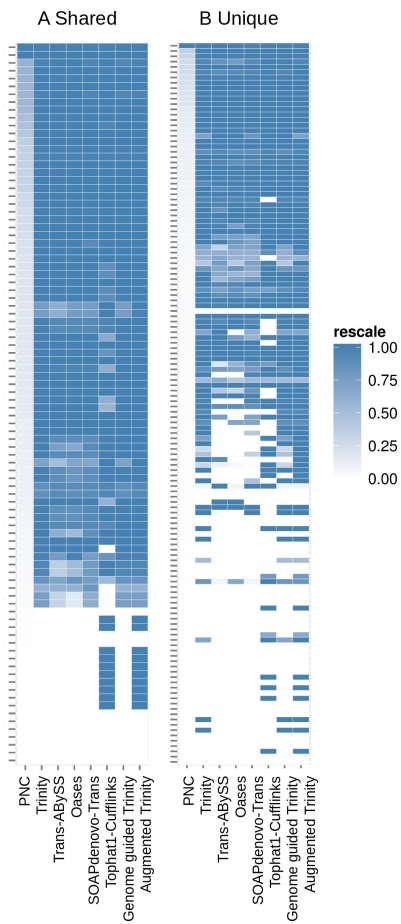


Figure 7: Heatmap analyses of % length recovery.

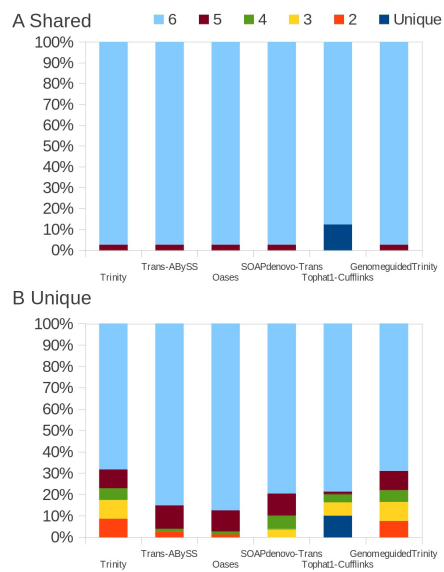


Figure 8: Intersection of recovered transcripts.

produced a set of unique transcripts or fragments, especially at lower levels of expression (Figure 2). Hence, we started by asking a question whether one can obtain a better transcriptome assembly when augmenting the *de novo* assembly with that from a genome-guided approach. While this was a reasonable question to ask, the presence of multiple tools, and hence errors associated with each of them, compounded the problem. Therefore, we started by finding out the efficiency of individual tools, the ones that are popularly used by the community, with the hope that we could choose from assemblers and combine the results from them without compounding additional errors in the final assembly.

A lower threshold for minimum fragment length allows one to retain valid assemblies (as demonstrated in Figure 3) at the expense of increasing errors. However, in our observation, the errors are comparatively lesser than the number of valid assemblies (Figure 4). The extent of mis-assembly by different assemblers was different. Oases and Trans-ABYSS resulted in more mis-assemblies than the other tools (Figure 4). We suspected that a large number of redundant transcripts produced by Oases and Trans-ABYSS were possibly mis-assembled. Interestingly, however, when we compared the mis-assembly statistics before and after redundancy removal, we found that Oases had more mis-assembly in the non-redundant regions of the transcriptome than Trans-ABYSS (Figure 4) pointing towards assembly of more number of chimeric transcripts.

Due to higher sub-sequence similarity in isoforms, which contain more shared regions than non-isoforms, the chances of mis-assembly are greater. The shared regions among transcripts also pose additional difficulty in discerning their true identity at the time of estimating recovery using mapping. We analyzed the shared and unique regions within isoforms separately in order to distinguish their recovery and underlying pnc patterns. All measures of pnc used for comparisons in this paper are based on the reads mapped to the MA as we were left with the option of remapping the reads to the assemblies in order to calculate the expression level, i.e. pnc in the absence of read tracking during transcriptome assembly. Re-mapping of reads is typically done using aligners that might result in multiple hits. This compels the user to arbitrarily assign the pnc to a transcript fragment, which may or may not be the same as the pnc estimated by an assembler. With simulated reads, where we knew the actual pnc of MA fragments, relationship between the actual (simulated) and estimated pnc using Megablast could be correlated. As expected, we found this to be true (Supplementary Figure 2). Based on this, we expected that the estimated pnc of transcript fragments by any assembler to be positively correlated with the actual pnc. In addition to the simulated dataset, we used the zebrafish hox gene cluster for transcript recovery analysis. Vertebrate Hox genes are known to be involved during development, are arranged in sets of uninterrupted clusters, and are in most cases expressed in a collinear fashion making it an ideal gene cluster candidate for our assembly analysis. We used RNA-seq reads from zebrafish to perform the assembly and derived assembled fragments related to the hox gene cluster to perform recovery analysis. We expected the shared regions had sequencing reads at a greater read depth than the unique regions. Indeed, we found this to be reflected in terms of a greater median pnc for the shared regions in the >50% recovery category (Figures 6 and 7).

N50 is an assembly attribute widely used to compare the quality of a transcriptome assembly. In the absence of the knowledge of actual length distribution in the sequenced dataset (transcripts sequenced), it is generally assumed that a higher N50 is correlated with a better assembly length-recovery/contiguity. We know that errors and redundancy in the transcriptome assembly affect its total size. In addition, the lengths of assembly fragments were also variable (e.g. Tophat1-Cufflinks produced more full length transcripts and Trinity produced more number of small fragments than the rest of the assemblers). Therefore, basing a quality metric on the total assembly size to benchmark the assembler, like what the N50 does, can be highly inaccurate. Instead, basing the quality metric on the expected size of the transcriptome (NT50) or regions of the transcriptome that is covered by sequencing reads, as $N_{(MA)}50$ suggests in simulated reads, tend to provide a more accurate benchmark. Indeed, we found that the $N_{(MA)}50$ to accurately reflect the recovery quotient of an assembler (Table 1). The reduction in $N_{(MA)}50$ for well-performing assemblers (Trinity, Genome guided Trinity and SOAPdenovo-Trans) when compared to that for the MA, was in proportion to the relative reduction in their assembly numbers in comparison to the number of MA fragments (Table 1). In addition to $N_{(MA)}50$, we found that the median, inter-quartile range, minimum, maximum and outliers for transcript assembly length were more useful in describing a transcriptome assembly.

Mis-assembly can occur as a result of sub-sequence similarity within reads, which manifests as highly branched nodes in a de Bruijn graph. This subsequence similarity, along with mismatches/errors in sequencing reads, can also cause spurious blast hits that are seen as outliers observed in the box and whisker plot for MA recovery, represented in Figure 3. Spurious blast hits due to the former tend to span from Megablast word size of 28bp onwards. We observed fewer outliers of the first kind in multi-kmer based approaches like Oases

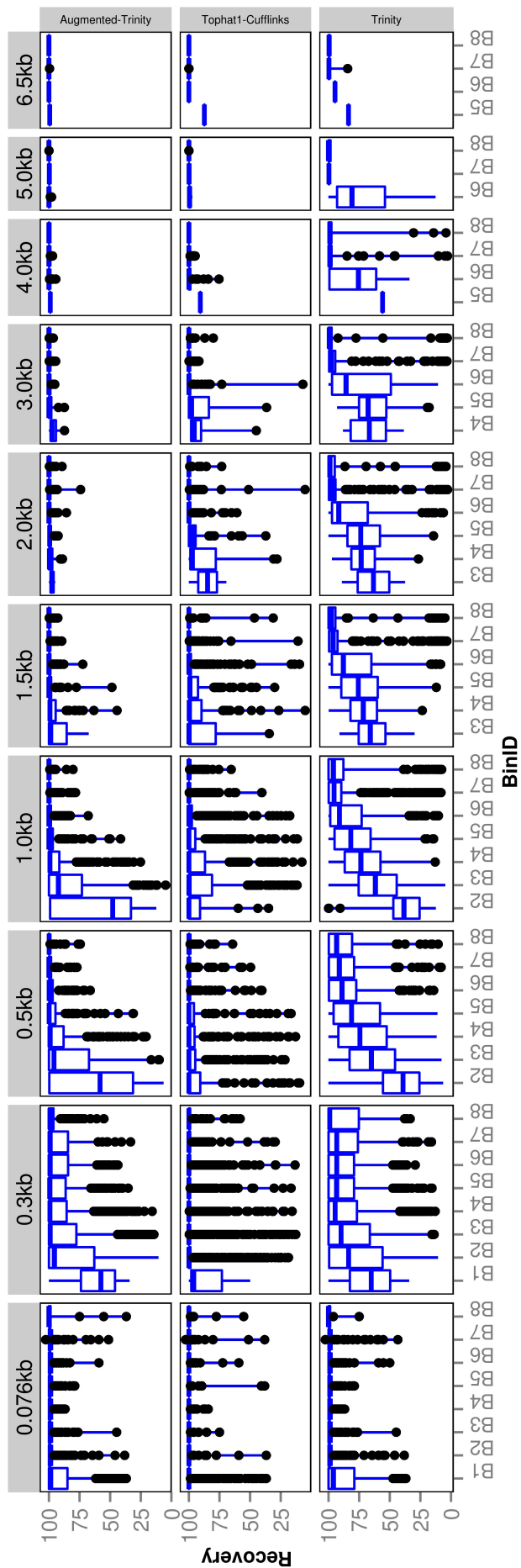


Figure 9: Intersection of recovered transcripts.

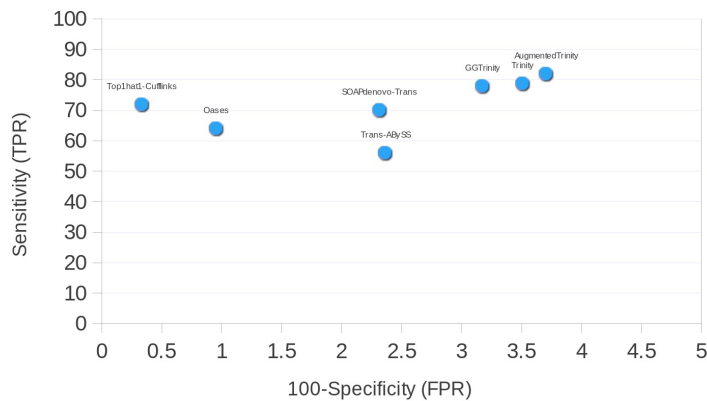


Figure 10: Intersection of recovered transcripts.

and Trans-ABYSS. SOAPdenovo-Trans also appears to contain fewer spurious blast hits, especially for the 76bp MA length category. It is known that SOAPdenovo algorithm chooses to discard a repetitive node if there is unequal read support on edges to and from that node, and only build parallel paths carrying the node if there are equal number of reads on either edges. Based on our observations of low redundancy in mapped assemblies in the 76bp MA length category (Figure 3) and higher % of assembly mapping correctly to a single MA fragment in the lower assembled fragment length categories (Figure 4), it is possible that SOAPdenovo-Trans discarded repetitive sequences from the assembly for these length categories. TransABYSS, prior to eliminating redundancy, showed a higher frequency for assembled fragments lengths > 200 bp (Figure 1A). The frequency of assembled fragments in this length range was much lower, post CD-HIT-EST (Figure 1B), suggesting the sequence redundancy in this range. Hence, we believe that there was relationship between redundancy and recovery of assembled fragments in our study. In our study, we found Trinity to perform best in transcript recovery across all expression levels (Figures 2 and 3). The median length recovery by Tophat1-Cufflinks was always $\sim 100\%$ (Figure 3). We chose to combine the Trinity assemblies with that from the Tophat1-Cufflinks assembly pipeline. This resulted in 1300 more transcript fragments corresponding to an cumulative increase of nearly 0.5million nt in length. The process resulted in an augmented assembly with even greater sensitivity and only minimally compromising its specificity, while maintaining the expression-based fragmented assembly structure of Trinity post- augmentation (Figure 10). The improved recovery post-augmentation proved that an integrative approach may be employed in recovering more transcript fragments, particularly when one has access to genome assembly in addition to RNA-seq reads.

Acknowledgement

The authors would like to thank Professor N. Yathindra for encouragement.

Funding

Research is funded by Department of Electronics and Information Technology, Government of India (Ref No:18(4)/2010-E-Infra., 31-03-2010) and Department of IT, BT and ST, Government of Karnataka, India (Ref No:3451-00-090-2-22) under the “Bio-IT Project”.

Author Contributions

Conceived the project: BP. Designed and analyzed the data: PJ and NMK. Wrote the paper: PJ, NMK & BP.

References

- Altschul SF, Gish W, Miller W, Myers EW, and Lipman DJ. 1990. Basic local alignment search tool. *J Mol Biol* 215:403-410.
- Biról I, Jackman SD, Nielsen CB, Qian JQ, Varhol R, Stazyk G, Morin RD, Zhao Y, Hirst M, Schein JE et al. . 2009. De novo transcriptome assembly with ABySS. *Bioinformatics* 25:2872-2877.
- Collins LJ, Biggs PJ, Voelckel C, and Joly S. 2008. An approach to transcriptome analysis of non-model organisms using short-read sequences. *Genome Inform* 21:3-14.

- Corredor-Adamez M, Welten MC, Spaink HP, Jeffery JE, Schoon RT, de Bakker MA, Bagowski CP, Meijer AH, Verbeek FJ, and Richardson MK. 2005. Genomic annotation and transcriptome analysis of the zebrafish (*Danio rerio*) *hox* complex with description of a novel member, *hox b 13a*. *Evol Dev* 7:362-375.
- DeRisi J, Penland L, Brown PO, Bittner ML, Meltzer PS, Ray M, Chen Y, Su YA, and Trent JM. 1996. Use of a cDNA microarray to analyse gene expression patterns in human cancer. *Nat Genet* 14:457-460.
- Egan AN, Schlueter J, and Spooner DM. 2012. Applications of next-generation sequencing in plant biology. *Am J Bot* 99:175-185.
- Gibbons JG, Janson EM, Hittinger CT, Johnston M, Abbot P, and Rokas A. 2009. Benchmarking next-generation transcriptome sequencing for functional and evolutionary genomics. *Mol Biol Evol* 26:2731-2744.
- Golub TR, Slonim DK, Tamayo P, Huard C, Gaasenbeek M, Mesirov JP, Coller H, Loh ML, Downing JR, Caligiuri MA et al. . 1999. Molecular classification of cancer: class discovery and class prediction by gene expression monitoring. *Science* 286:531-537.
- Grabherr MG, Haas BJ, Yassour M, Levin JZ, Thompson DA, Amit I, Adiconis X, Fan L, Raychowdhury R, Zeng Q et al. . 2011. Full-length transcriptome assembly from RNA-Seq data without a reference genome. *Nat Biotechnol* 29:644-652.
- Griebel T, Zacher B, Ribeca P, Raineri E, Lacroix V, Guigo R, and Sammeth M. 2012. Modelling and simulating generic RNA-Seq experiments with the flux simulator. *Nucleic Acids Res* 40:10073-10083.
- Gruenheit N, Deusch O, Esser C, Becker M, Voelckel C, and Lockhart P. 2012. Cutoffs and k-mers: implications from a transcriptome study in allopolyploid plants. *BMC Genomics* 13:92.
- Kim D, Pertea G, Trapnell C, Pimentel H, Kelley R, and Salzberg SL. 2013. TopHat2: accurate alignment of transcriptomes in the presence of insertions, deletions and gene fusions. *Genome Biol* 14:R36.
- Kuraku S, and Meyer A. 2009. The evolution and maintenance of Hox gene clusters in vertebrates and the teleost-specific genome duplication. *Int J Dev Biol* 53:765-773.
- Langmead B. 2010. Aligning short sequencing reads with Bowtie. *Curr Protoc Bioinformatics* Chapter 11:Unit 11 17.
- Li R, Yu C, Li Y, Lam TW, Yiu SM, Kristiansen K, and Wang J. 2009. SOAP2: an improved ultrafast tool for short read alignment. *Bioinformatics* 25:1966-1967.
- Li R, Zhu H, Ruan J, Qian W, Fang X, Shi Z, Li Y, Li S, Shan G, Kristiansen K et al. . 2010. De novo assembly of human genomes with massively parallel short read sequencing. *Genome Res* 20:265-272.
- Li W, and Godzik A. 2002. Discovering new genes with advanced homology detection. *Trends Biotechnol* 20:315-316.
- Martin JA, and Wang Z. 2011. Next-generation transcriptome assembly. *Nat Rev Genet* 12:671-682.
- Mitchell W. 2011. Natural products from synthetic biology. *Curr Opin Chem Biol* 15:505-515.
- Mortazavi A, Williams BA, McCue K, Schaeffer L, and Wold B. 2008. Mapping and quantifying mammalian transcriptomes by RNA-Seq. *Nat Methods* 5:621-628.
- Mundry M, Bornberg-Bauer E, Sammeth M, and Feulner PG. 2012. Evaluating characteristics of de novo assembly software on 454 transcriptome data: a simulation approach. *PLoS One* 7:e31410.
- Nagarajan N, and Pop M. 2013. Sequence assembly demystified. *Nat Rev Genet* 14:157-167.
- Ozsolak F, and Milos PM. 2011. RNA sequencing: advances, challenges and opportunities. *Nat Rev Genet* 12:87-98.
- Roberts A, Pimentel H, Trapnell C, and Pachter L. 2011. Identification of novel transcripts in annotated genomes using RNA-Seq. *Bioinformatics* 27:2325-2329.
- Robertson G, Schein J, Chiu R, Corbett R, Field M, Jackman SD, Mungall K, Lee S, Okada HM, Qian JQ et al. . 2010. De novo assembly and analysis of RNA-seq data. *Nat Methods* 7:909-912.
- Salzberg SL, Sommer DD, Puiu D, and Lee VT. 2008. Gene-boosted assembly of a novel bacterial genome from very short reads. *PLoS Comput Biol* 4:e1000186.
- Schena M, Shalon D, Davis RW, and Brown PO. 1995. Quantitative monitoring of gene expression patterns with a complementary DNA microarray. *Science* 270:467-470.
- Schena M, Shalon D, Heller R, Chai A, Brown PO, and Davis RW. 1996. Parallel human genome analysis: microarray-based expression monitoring of 1000 genes. *Proc Natl Acad Sci U S A* 93:10614-10619.
- Schulz MH, Zerbino DR, Vingron M, and Birney E. 2012. Oases: robust de novo RNA-seq assembly across the dynamic range of expression levels. *Bioinformatics* 28:1086-1092.
- Shendure J, and Lieberman Aiden E. 2012. The expanding scope of DNA sequencing. *Nat Biotechnol* 30:1084-1094.
- Simon SA, Zhai J, Nandety RS, McCormick KP, Zeng J, Mejia D, and Meyers BC. 2009. Short-read sequencing technologies for transcriptional analyses. *Annu Rev Plant Biol* 60:305-333.
- Simpson JT, Wong K, Jackman SD, Schein JE, Jones SJ, and Birol I. 2009. ABySS: a parallel assembler for short read sequence data. *Genome Res* 19:1117-1123.

- Toth AL, Varala K, Newman TC, Miguez FE, Hutchison SK, Willoughby DA, Simons JF, Egholm M, Hunt JH, Hudson ME et al. . 2007. Wasp gene expression supports an evolutionary link between maternal behavior and eusociality. *Science* 318:441-444.
- Trapnell C, Pachter L, and Salzberg SL. 2009. TopHat: discovering splice junctions with RNA-Seq. *Bioinformatics* 25:1105-1111.
- Trapnell C, Roberts A, Goff L, Pertea G, Kim D, Kelley DR, Pimentel H, Salzberg SL, Rinn JL, and Pachter L. 2012. Differential gene and transcript expression analysis of RNA-seq experiments with TopHat and Cufflinks. *Nat Protoc* 7:562-578.
- Trapnell C, Williams BA, Pertea G, Mortazavi A, Kwan G, van Baren MJ, Salzberg SL, Wold BJ, and Pachter L. 2010. Transcript assembly and quantification by RNA-Seq reveals unannotated transcripts and isoform switching during cell differentiation. *Nat Biotechnol* 28:511-515.
- TrinityTeam. 2013. Genome-guided Trinity. http://trinityrnaseq.sourceforge.net/genome_guided_trinity.html
- Waern K, Nagalakshmi U, and Snyder M. 2011. RNA sequencing. *Methods Mol Biol* 759:125-132.
- Wang Z, Gerstein M, and Snyder M. 2009. RNA-Seq: a revolutionary tool for transcriptomics. *Nat Rev Genet* 10:57-63.
- Wu TD, and Nacu S. 2010. Fast and SNP-tolerant detection of complex variants and splicing in short reads. *Bioinformatics* 26:873-881.
- Zerbino DR, and Birney E. 2008. Velvet: algorithms for de novo short read assembly using de Bruijn graphs. *Genome Res* 18:821-829.

Figure Legends

Figure 1: Frequency distribution of lengths (bp) of MA & assembled transcript fragments before (A) and after (B) CDHit-EST.

Figure 2: The number of recovered MA fragments in different expression bins.

The recovery of MA fragments by six assemblers was estimated across eight expression level categories (B1 - B8) binned by per-nucleotide-coverage (pnc). The recovered fragments are presented as unique to an assembler or as an overlap between 2, 3, 4, or 5, or all the six assemblers for each expression bin.

Figure 3: Recovered length (%) of MA fragments.

MA fragments were binned into different length categories (≤ 76 bp, 76-300bp, 300-500bp, 500bp-1kb, 1-1.5kb, 1.5-2kb, 2-3kb, 3-4kb, 4-5kb, 5-6.5kb), and the length recovered for each assembler across expression bins (B1-B8) was visualized separately for each MA length bin. The black dots represent the outliers, the boxes represent the 25% (Q1)-75% (Q3) interquartile range (IQR), the middle line in the boxes represents the median, and the blue solid lines represent the whiskers from these boxes till

the minimum/maximum of the length range. Outliers fall below $Q1 - 1.5 \hat{A} \sim IQR$ or above $Q3 + 1.5 \hat{A} \sim IQR$. See Supplementary Methods for script used to generate the plot.

Figure 4: Assembly mapping statistics

The assembled fragments were classified as $>90\%$, between 60-90% and $<60\%$ categories based on the fraction mapped to a single MA fragment, before (A) and after (B) removal of redundancy.

Figure 5: Isoform recovery statistics.

Recovery was estimated for the number of exons per isoform in different (0%, $>0-20\%$, $>20-40\%$, $>40-60\%$, $>60-80\%$ and $>80-100\%$) recovery categories. The median pnc of isoforms for each of these categories was also estimated for each assembler.

Figure 6: Recovery of transcripts in the unique and shared regions of hox gene cluster in zebrafish.

The unique and shared regions of hox gene cluster from zebrafish *Danio rerio* with a minimum per-nucleotide coverage (pnc) of 1 were extracted. The recovery was measured for these regions in the 0%, 0-50% and 50-100% recovery categories.

Figure 7: Heatmap analyses of %length recovery of shared and unique transcript regions of the zebrafish hox gene cluster.

The transcript regions were ranked in a descending order of their PNCs.

Figure 8: Intersection histogram of recovered transcripts from the shared and unique regions of the zebrafish hox gene cluster

Figure 9: Recovered length (%) of model assembly (MA) fragments after augmenting with Trinity-assembled fragments.

Mapping of Trinity assembled transcript fragments with the transcripts assembled by Tophat1-Cufflinks. The transcript regions unique to Tophat1-Cufflinks were used to augment the Trinity assembly. The length recovery was visualized in the same manner as described in Figure 3.

Figure 10: ROC curve for transcriptome assemblers.

The sensitivity (TPR) was estimated as % total length recovered for each assembler out of the total MA size. The FPR (100-specificity) was estimated as the % assembled fragments that did not map to the MA fragments. For Tophat1-Cufflinks assembler, and the unique regions to Tophat1-Cufflinks used to augment Trinity, the mapping was performed with the TAIR10 transcripts.



Figure S1: Expression level bin assignment for MA fragments with varying length categories.

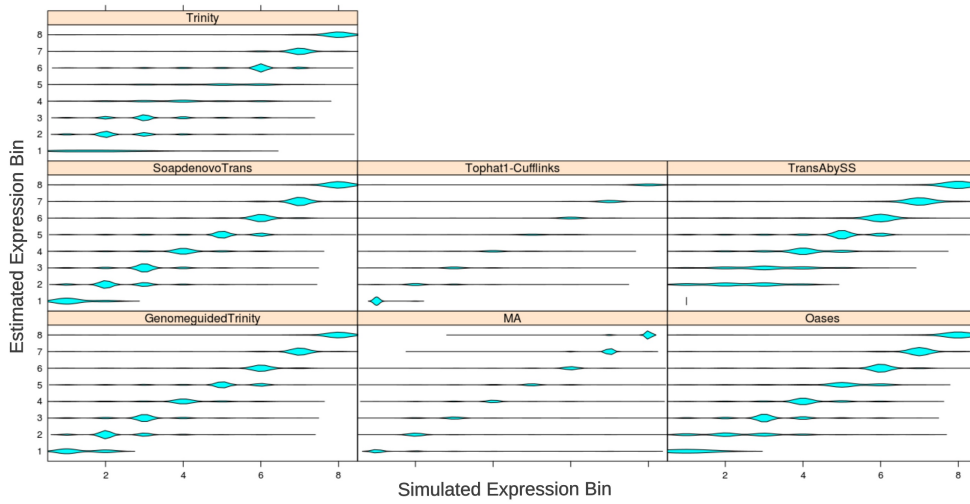


Figure S2: Correlation between simulated and estimated expression level binning.